AIP | Journal of Applied Physics

Lattice and grain-boundary diffusions of boron atoms in BaSi2 epitaxial films on Si(111)

K. Nakamura, M. Baba, M. Ajmal Khan, W. Du, M. Sasase et al.

Citation: J. Appl. Phys. **113**, 053511 (2013); doi: 10.1063/1.4790597
View online: http://dx.doi.org/10.1063/1.4790597
View Table of Contents: http://jap.aip.org/resource/1/JAPIAU/v113/i5
Published by the American Institute of Physics.

Lattice and grain-boundary diffusions of boron atoms in $BaSi_2$ epitaxial films on Si(111)

K. Nakamura,[1] M. Baba,[1] M. Ajmal Khan,[1] W. Du,[1] M. Sasase,[2] K. O. Hara,[3] N. Usami,[3,4] K. Toko,[1] and T. Suemasu[1,4,a)]

[1]*Institute of Applied Physics, University of Tsukuba, Tsukuba, Ibaraki 305-8573, Japan*
[2]*The Wakasa Wan Energy Research Center, Tsuruga, Fukui 914-0192, Japan*
[3]*Institute for Materials Research, Tohoku University, Sendai 980-8577, Japan*
[4]*Japan Science and Technology Agency, CREST, Tokyo 102-0075, Japan*

(Received 5 November 2012; accepted 22 January 2013; published online 6 February 2013)

A 180-nm-thick boron (B) layer was deposited on a 300-nm-thick *a*-axis-oriented $BaSi_2$ epitaxial film grown by molecular beam epitaxy on Si(111) and was annealed at different temperatures in ultrahigh vacuum. The depth profiles of B were investigated using secondary ion mass spectrometry (SIMS) with O^{2+}, and the diffusion coefficients of B were evaluated. The B profiles were reproduced well by taking both the lattice and the grain boundary (GB) diffusions into consideration. The cross-sectional transmission electron microscopy (TEM) image revealed that the GBs of the $BaSi_2$ film were very sharp and normal to the sample surface. The plan-view TEM image exhibited that the grain size of the $BaSi_2$ film was approximately 0.6 μm. The temperature dependence of lattice and GB diffusion coefficients was derived from the SIMS profiles, and their activation energies were found to be 4.6 eV and 4.4 eV, respectively. © *2013 American Institute of Physics*.
[http://dx.doi.org/10.1063/1.4790597]

I. INTRODUCTION

Photovoltaic cell production has been increasing and its market continues to expand rapidly. Approximately 90% of solar cells are made from Si, because Si is an abundant and well-known material in the semiconductor industry. However, the optical absorption layers of crystalline Si (c-Si) solar cells tend to be much thicker than the conventional thin-film solar cells, such as $CuInGaSe_2$ (CIGS), because the optical absorption coefficient is much smaller for c-Si. Therefore, other Si-based materials for high-efficiency thin-film solar cells are of great interest. Among such materials, we have been focusing on semiconducting orthorhombic $BaSi_2$, which has particularly favorable characteristics for solar cell applications. $BaSi_2$ has the bandgap of approximately 1.3 eV and a very large optical absorption coefficient, reaching $3 \times 10^4\,cm^{-1}$ at 1.5 eV experimentally.[1–3] *a*-Axis-oriented $BaSi_2$ can be grown epitaxially on Si(111) and Si(001) substrates.[4–10] Recently, we have successfully achieved large photoresponsivity and internal quantum efficiency exceeding 70% in *a*-axis-oriented $BaSi_2$ epitaxial layers grown by molecular beam epitaxy (MBE).[11–14] Excess carrier recombination mechanisms in $BaSi_2$ have also been studied.[15] These results have spurred interest in this material.

The basic structure of a solar cell is a *p-n* junction. Therefore, control of the conductivity of $BaSi_2$ by impurity doping is required. The carrier concentration of undoped *n*-$BaSi_2$ is approximately $5 \times 10^{15}\,cm^{-3}$.[1] According to Imai and Watanabe,[16] the substitution of Si in the $BaSi_2$ lattice is more favorable than the substitution of Ba from an energetic point of view by first-principles calculation. In our previous works, the electron concentration of Sb-doped $BaSi_2$ was controlled in the range between 10^{16} and $10^{20}\,cm^{-3}$ at room temperature (RT). In contrast, Al- and In-doped $BaSi_2$ show *p*-type conductivity, but the hole concentration was limited up to $3 \times 10^{17}\,cm^{-3}$.[17] Very recently, we have achieved the hole concentration exceeding $10^{19}\,cm^{-3}$ in B-doped $BaSi_2$.[18] The hole concentration of B-doped $BaSi_2$ was controlled in the range between 10^{16} and $10^{20}\,cm^{-3}$ at RT. Thus, B is considered a suitable *p*-type dopant. However, there has been no report on the diffusion coefficient of B in $BaSi_2$. Diffusion coefficient is a decisive parameter that will affect the steepness of a *p-n* junction.

In this study, we aim to evaluate the lattice diffusion coefficient of B using secondary ion mass spectrometry (SIMS) measurement. Grain boundary (GB) diffusion coefficient was also investigated because the plan-view and the cross-sectional transmission electron microscopy (TEM) images revealed the presence of GBs in the *a*-axis-oriented $BaSi_2$ epitaxial layer on Si(111). This is due to the sixfold symmetry caused by three epitaxial variants rotated by 120° with respect to each other around the surface normal.[6,19]

II. EXPERIMENTAL METHOD

A two-step growth method was adopted, that is, the reactive deposition epitaxy (RDE; Ba deposition on hot Si) for $BaSi_2$ template layers and followed by the molecular beam epitaxy (MBE; codeposition of Ba and Si on Si) at 600 °C to form 300 nm-thick *a*-axis-oriented $BaSi_2$ epitaxial films on Si(111). The details of the growth procedure have been previously described.[6,19] The grown samples were post-annealed at 850 °C for 10 min in ultrahigh vacuum (UHV). This high-temperature annealing was performed so that the crystal quality of $BaSi_2$ film remains unchanged by the annealing for B

a)Author to whom correspondence should be addressed. Electronic mail: suemasu@bk.tsukuba.ac.jp. Tel./Fax: +81-29-853-5111.

diffusion. Then, an approximately 180-nm-thick B layer was evaporated at RT. This sample was cut into several pieces and annealed at different temperatures of 775, 800, and 825 °C for 5, 1, and 0.5 h, respectively, in UHV. These temperatures are much higher than the MBE growth temperature of 600 °C. The sample preparation is summarized in Table I. We investigated the depth profiles of B in the $BaSi_2$ using SIMS measurement with O^{2+} and evaluated the lattice and GB diffusion coefficients. In order to investigate the grain size of $BaSi_2$ and the GBs, both plan-view and cross-sectional TEM observations were performed.

III. RESULTS AND DISCUSSIONS

Figure 1(a) shows the plan-view bright-field (BF) TEM image of the post-annealed *a*-axis-oriented $BaSi_2$ epitaxial film. The incident electron beam was almost parallel to the $BaSi_2$[100] zone axis, but it was slightly tilted for the GBs to be seen clearly. Note that approximately 120°, sharp GBs are present, and these GBs consist mostly of $BaSi_2${011} planes. Detailed discussions about the GBs were given in our previous report.[19] We can see that the grain size of the post-annealed $BaSi_2$ was approximately 0.6 μm. The cross-sectional TEM image of this sample, shown in Fig. 1(b), shows that the GBs of the $BaSi_2$ film were very sharp and normal to the substrate surface, namely in the $BaSi_2$[100] direction. On the basis of these cross-sectional and plan-view TEM images, we concluded that the *a*-axis-oriented $BaSi_2$ film is composed of columnar-shaped $BaSi_2$ grains.

We then discussed the diffusion coefficients of B in $BaSi_2$. The depth profiles of B are shown in Fig. 2, where the B concentrations were normalized by the B concentration in the B layer, C_0, described later. Reference samples with a controlled number of B doped in $BaSi_2$ have not yet been prepared but it is necessary to precisely determine the impurity concentration by SIMS. Although the exact B concentrations could not be obtained, it does not affect the analyses afterwards. In order to fit the experimental SIMS profiles, both lattice and GB diffusions were taken into consideration because we can see clear GBs in the $BaSi_2$ films as shown in Figs. 1(a) and 1(b). We adopted Eqs. (1) and (2) for fitting the SIMS profiles of B atoms. The concentration distribution $C(x, t)$ of impurity atom due to the lattice diffusion is given by Eq. (1)

$$C(x,t) = C_0 \,\mathrm{erfc}(x/2\sqrt{D_l t}), \tag{1}$$

where $x = 0$ is set at the B/$BaSi_2$ interface, and C_0 is the B concentration at $x = 0$, D_l is the lattice diffusion coefficient, and t is the annealing duration. On the other hand, the concentration distribution due to GB diffusion follows Eq. (2)[20–22]

$$s\delta D_{\mathrm{GB}} = 1.322(D_l/t)^{1/2}(-\partial \ln C(x,t)/\partial x^{6/5})^{-5/3}, \tag{2}$$

TABLE I. Sample preparation: annealing temperature and duration for post-anneal and for B diffusion in UHV.

Sample	Post anneal (°C/min)	Diffusion for B diffusion (°C/h)
A	850/10	775/5
B	850/10	800/1
C	850/10	825/0.5

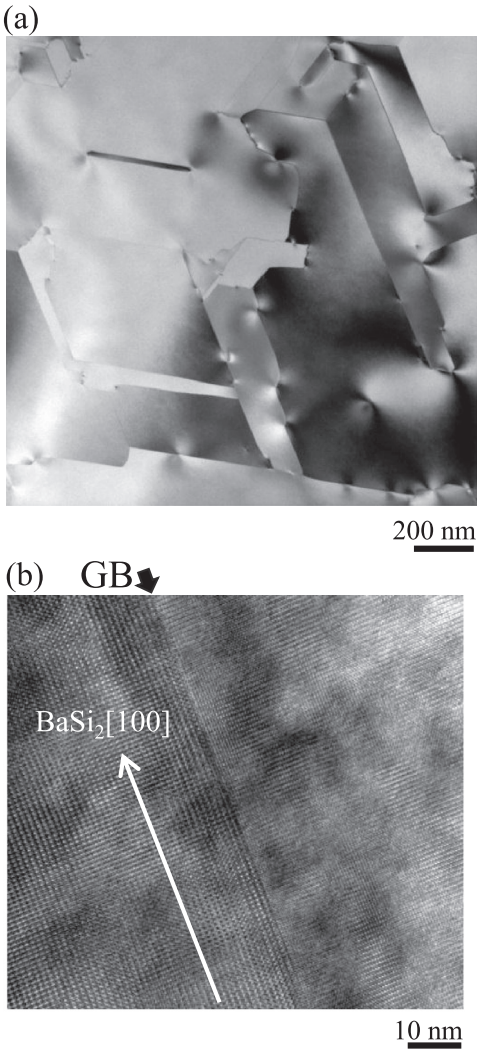

FIG. 1. (a) Plan-view BF TEM image and (b) cross-sectional TEM images for the post-annealed $BaSi_2$ film. In the plan-view TEM, the incident electron beam was almost parallel to the $BaSi_2$[100] zone axis but was slightly tilted for the GBs to be seen clearly.

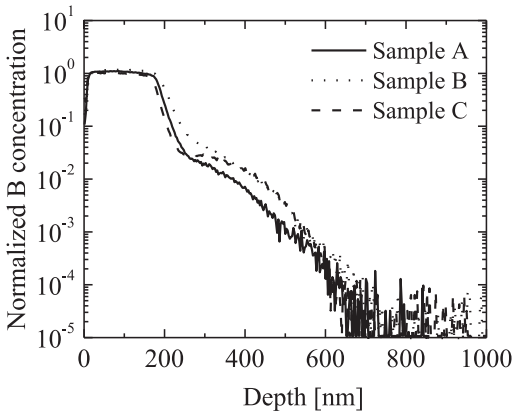

FIG. 2. Normalized SIMS depth profiles of B for samples A-C, annealed at different temperatures.

where s is the segregation factor, δ is the grain boundary width, and D_{GB} is the GB diffusion coefficient. Equation (2) corresponds to the Harrison Type-B kinetics regime which refers to a situation where the average lattice diffusion length of the diffusion atoms is less than the grain size.[22–24] The grain size of the post-annealed $BaSi_2$ was approximately 0.6 μm as shown in Fig. 1(a). This value is much larger than the diffusion length of B in the post-annealed $BaSi_2$ film, meaning that Eq. (2) is valid in this work. Figure 3 shows an example of the measured and simulated SIMS profiles of B for sample B. Annealing for B diffusion was performed at 800 °C for 1 h. The experimentally obtained depth profile of B was reproduced well with Eqs. (1) and (2). We should note here that there are four regions in Fig. 3, that is, the B capping layer region, the lattice diffusion region (broken line), the GB diffusion region (dotted line), and the Si substrate. The SIMS profile in the region deeper than 500 nm from the surface could not be explained well by the GB diffusion. This is because the interface of undoped $BaSi_2$/Si(111) substrate was located around there. Similar fittings were performed for samples A and C to evaluate the diffusion coefficients.

The Arrhenius plots for the obtained D_l and $s\delta D_{GB}$ are shown in Figs. 4(a) and 4(b), respectively. The gradient of the Arrhenius plots in these figures revealed that the activation energies of lattice and GB diffusions are 4.6 eV and 4.4 eV for B atoms, respectively. D_l in single crystal Si and D_{GB} in poly crystalline Si for $B(B_2H_6)$ are shown in Fig. 5.[25,26] D_l and sD_{GB} for Ni, Si, As atoms in the Ni_2Si thin film and Co, Si atoms in the $CoSi_2$ bulk are also shown for comparison.[27–32] The GB width δ for the $BaSi_2$ film was set to 0.5 nm because it is usually taken as 0.5 nm in GB diffusion studies.[33,34] The GB in the $BaSi_2$ epitaxial film is so sharp as shown in Fig. 1(b) that this assumption seems reasonable. Although the segregation factor s cannot be determined for $BaSi_2$ in this work, it was reported that s is equal to 1 for self-diffusion like GB diffusion of Ni in Ni_2Si.[24] The values of D_l and sD_{GB} for B in the $BaSi_2$ film seem valid because they are not far from those of some atoms in Si and silicides.

Here, we discuss the diffusion length of B atoms along the GBs in such a case that we form a B-doped p-$BaSi_2$/undoped n-$BaSi_2$ junction on a metal electrode and perform rapid thermal annealing (RTA) to activate B atoms in the $BaSi_2$. RTA treatment at 800 °C for 2 min was known to be an effective means to activate B atoms.[18] During the RTA, the B atoms were supposed to diffuse faster along the GBs

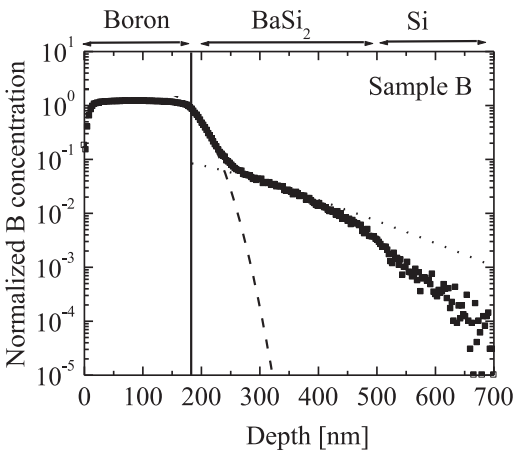

FIG. 3. Measured and simulated SIMS profiles of B for sample B, annealed at 800 °C for 1 h.

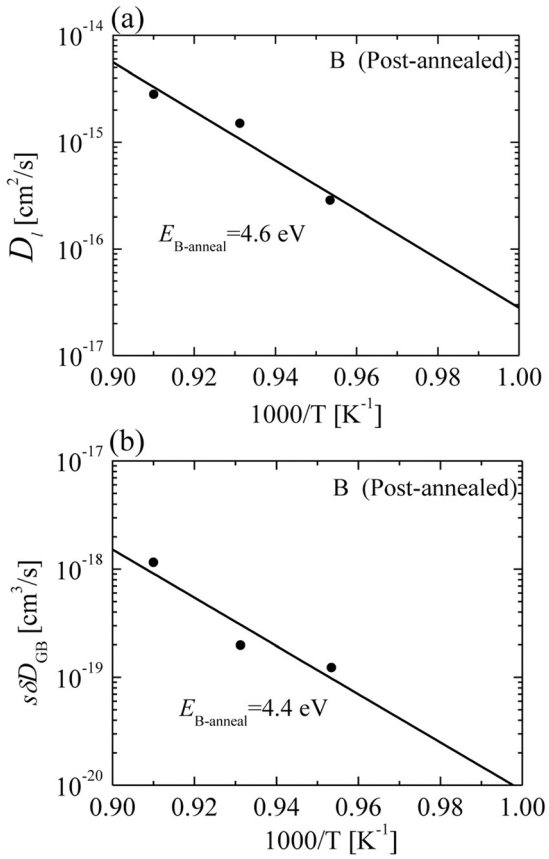

FIG. 4. Arrhenius plots of (a) D_l and (b) $s\delta D_{GB}$ of B in $BaSi_2$.

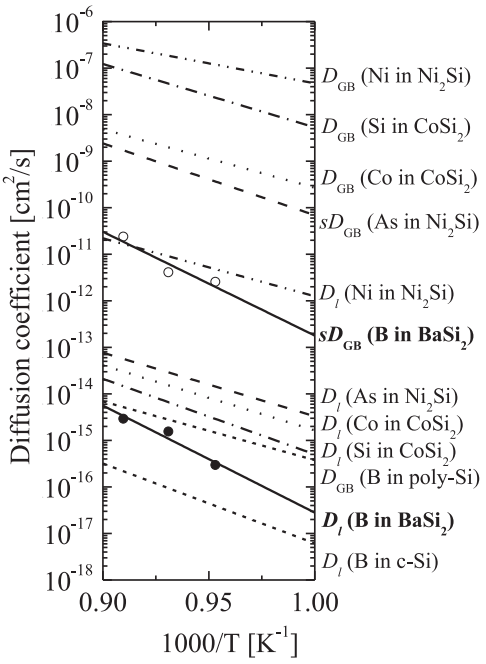

FIG. 5. Arrhenius plots of D_l and sD_{GB} of B in $BaSi_2$ and those of some atoms in crystalline Si and silicide materials.[25–32] GB width δ is set to 0.5 nm for each silicide films including $BaSi_2$.

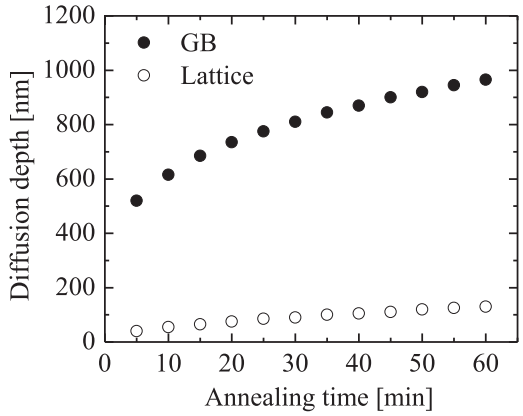

FIG. 6. Estimated B diffusion lengths annealed at 800 °C in *a*-axis-oriented $BaSi_2$ due to lattice and GB diffusions. The diffusion length was determined to be the depth, where the B concentration becomes 10^4 times smaller than that at the B source/$BaSi_2$ interface ($x = 0$).

because sD_{GB} is 10^4 times larger than D_l for B at around 800 °C in the $BaSi_2$ film. The carrier concentration of undoped *n*-$BaSi_2$ is approximately $10^{16}\,cm^{-3}$.[1] Thus, the diffused B concentration should be less than $10^{16}\,cm^{-3}$ at the diffusion front edge provided that the activation rate of B is 100%; otherwise the B-doped GBs will reach the electrode and work as leakage pathways. Assuming that the B concentration in the B-doped *p*-$BaSi_2$ is $10^{20}\,cm^{-3}$, the concentration of B diffused into undoped *n*-$BaSi_2$ should be 10^4 times smaller than that of B-doped layer. The estimated GB diffusion length of B, where the B concentration becomes as large as $10^{16}\,cm^{-3}$, is shown in Fig. 6. The GB diffusion length of B is predicted to be about 520 nm for RTA treatment at 800 °C for 5 min. Therefore, the $BaSi_2$ optical absorption layer thickness should be much more than 500 nm in a $BaSi_2$ *pn* junction solar cell structure.

IV. SUMMARY

The lattice and GB diffusion coefficients of B atoms were evaluated using the *a*-axis-oriented $BaSi_2$ epitaxial film capped with B layer. The cross-sectional and plan-view TEM observations showed that the 0.6-μm-sized grains were separated by very sharp GBs running normal to the sample surface in the post-annealed $BaSi_2$ film. The SIMS depth profiles of B atoms were reproduced relatively well by taking both the lattice and GB diffusions into consideration. The activation energy of lattice diffusion of B is 4.6 eV while the GB diffusion is 4.4 eV.

ACKNOWLEDGMENTS

The authors thank Mr. Saito and Dr. Yoshizawa of the National Institute of Advanced Industrial Science and Technology for TEM observations. This work was supported in part by CREST of JST.

[1]K. Morita, Y. Inomata, and T. Suemasu, Thin Solid Films **508**, 363 (2006).
[2]D. B. Migas, V. L. Shaposhnikov, and V. E. Borisenko, Phys. Status Solidi B **244**, 2611 (2007).
[3]K. Toh, T. Saito, and T. Suemasu, Jpn. J. Appl. Phys. Part 1 **50**, 068001 (2011).
[4]R. A. Mckee, F. J. Walker, J. R. Conner, E. D. Specht, and D. E. Zelmon, Appl. Phys. Lett. **59**, 782 (1991).
[5]R. A. Mckee and F. J. Walker, Appl. Phys. Lett. **63**, 2818 (1993).
[6]Y. Inomata, T. Nakamura, T. Suemasu, and F. Hasegawa, Jpn. J. Appl. Phys. Part 2 **43**, L478 (2004).
[7]K. O. Hara, N. Usami, K. Toh, K. Toko, and T. Suemasu, Jpn. J. Appl. Phys. Part 1 **51**, 10NB06 (2012).
[8]M. Baba, K. Nakamura, W. Du, M. Ajmal Khan, S. Koike, K. Toko, and T. Suemasu, Jpn. J. Appl. Phys. Part 1 **51**, 098003 (2012).
[9]K. Toh, K. O. Hara, N. Usami, N. Saito, N. Yoshizawa, K. Toko, and T. Suemasu, J. Cryst. Growth **345**, 16 (2012).
[10]K. Toh, K. O. Hara, N. Usami, N. Saito, N. Yoshizawa, K. Toko, and T. Suemasu, Jpn. J. Appl. Phys. Part 1 **51**, 095501 (2012).
[11]W. Du, M. Suzuno, M. A. Khan, K. Toh, M. Baba, K. Nakamura, K. Toko, N. Usami, and T. Suemasu, Appl. Phys. Lett. **100**, 152114 (2012).
[12]Y. Matsumoto, D. Tsukada, R. Sasaki, M. Takeishi, and T. Suemasu, Appl. Phys. Express **2**, 021101 (2009).
[13]D. Tsukada, Y. Matsumoto, R. Sasaki, M. Takeishi, T. Saito, N. Usami, and T. Suemasu, Appl. Phys. Express **2**, 051601 (2009).
[14]T. Saito, Y. Matsumoto, M. Suzuno, M. Takeishi, R. Sasaki, N. Usami, and T. Suemasu, Appl. Phys. Express **3**, 021301 (2010).
[15]K. O. Hara, N. Usami, K. Toh, M. Baba, K. Toko, and T. Suemasu, J. Appl. Phys. **112**, 083108 (2012).
[16]Y. Imai and A. Watanabe, Intermetallics **15**, 1291 (2007).
[17]M. Kobayashi, Y. Matsumoto, Y. Ichikawa, D. Tsukada, and T. Suemasu, Appl. Phys. Express **1**, 051403 (2008).
[18]M. Ajmal Khan, K. O. Hara, K. Nakamura, W. Du, M. Baba, K. Toh, M. Suzuno, K. Toko, N. Usami, and T. Suemasu, J. Cryst. Growth.
[19]M. Baba, K. Toh, K. Toko, N. Saito, N. Yoshizawa, K. Jiptner, T. Sekiguchi, K. O. Hara, N. Usami, and T. Suemasu, J. Cryst. Growth **348**, 75 (2012).
[20]A. D. Le Claire, Br. J. Appl. Phys. **14**, 351 (1963).
[21]R. T. P. Whipple, Philos. Mag. **45**, 1225 (1954).
[22]I. V. Belova and G. E. Murch, Philos. Mag. **89**, 665 (2009).
[23]L. G. Harrison, Trans. Faraday Soc. **57**, 1191 (1961).
[24]I. V. Belova, T. Fiedler, N. Kulkarni, and G. E. Murch, Philos. Mag. **92**, 1748 (2012).
[25]J. C. M. Hwang, P. S. Ho, J. E. Lewis, and D. R. Campbell, J. Appl. Phys. **51**, 1576 (1980).
[26]S. Horiuchi and R. Blanchard, Solid-State Electron. **18**, 529 (1975).
[27]T. Barge, S. Poize, J. Bemardini, and P. Gas, Appl. Surf. Sci. **53**, 180 (1991).
[28]T. Barge, Ph. D Thesis, Universite Aix-Marseille III, 1993.
[29]O. Thomas, P. Gas, A. Charai, F. M. D'Heurle, F. K. LeGoues, A. Michel, and G. Scilla, J. Appl. Phys. **64**, 2973 (1988).
[30]T. Barge, P. Gas, and F. M. d'Heurle, J. Mater. Res. **10**, 1134 (1995).
[31]I. Blum, A. Portavoce, D. Mangelinck, R. Daineche, K. Hoummada, J. L. Lábár, V. Carron, and J. Bernardini, Microelectron. Eng. **87**, 263 (2010).
[32]J. C. Ciccariello, S. Poize, and P. Gas, J. Appl. Phys. **67**, 3315 (1990).
[33]I. Kaur and W. Gust, *Fundamentals of Grain and Interphase Boundary Diffusion* (Ziegler, Stuttgart, 1988).
[34]Y. Mishin, C. Herzig, J. Bernardini, and W. Gust, Int. Mater. Rev. **42**, 155 (1997).